Steel and Composite Structures, *Vol. 21*, *No. 3* (*2016*) *479-500*
DOI: http://dx.doi.org/10.12989/scs.2016.21.3.479

Influence of seismic design rules on the robustness of steel moment resisting frames

David Cassiano [1a], Mario D'Aniello [*1], Carlos Rebelo [1b],
Raffaele Landolfo [2c] and Luís S. da Silva [1d]

[1] *ISISE, University of Coimbra, Polo II – R. Luís Reis Santos, 3030-788 Coimbra, Portugal*
[2] *Department of Structures for Engineering and Architecture, University of Naples "Federico II", via Forno Vecchio, 36 – Napoli 80134, Italy*

(*Received October 30, 2015, Revised February 26, 2016, Accepted April 30, 2016*)

Abstract. Seismic design criteria allow enhancing the structural ductility and controlling the damage distribution. Therefore, detailing rules and design requirements given by current seismic codes might be also beneficial to improve the structural robustness. In this paper a comprehensive parametric study devoted to quantifying the effectiveness of seismic detailing for steel Moment Resisting Frames (MRF) in limiting the progressive collapse under column loss scenarios is presented and discussed. The overall structural performance was analysed through nonlinear static and dynamic analyses. With this regard the following cases were examined: (i) MRF structures designed for wind actions according to Eurocode 1; (ii) MRF structures designed for seismic actions according to Eurocode 8. The investigated parameters were (i) the number of storeys; (ii) the interstorey height; (iii) the span length; (iv) the building plan layout; and (v) the column loss scenario. Results show that structures designed according to capacity design principles are less robust than wind designed ones, provided that the connections have the same capacity threshold in both cases. In addition, the numerical outcomes show that both the number of elements above the removed column and stiffness of beams are the key parameters in arresting progressive collapse.

Keywords: robustness; progressive collapse; pushdown; dynamic analysis; seismic design; MRF

1. Introduction

Seismic design rules currently implemented in modern codes (e.g., the EN 1998-1) aim at conceiving structures with adequate local and global ductility to guarantee the formation of an overall dissipative mechanism. This implies that dissipative zones (e.g., the beams in case of moment resisting frames) should be able to develop plastic hinges rotating until the collapse mechanism is completely developed, without reducing their moment capacity, thus assuring the qrequired redistribution of bending moments. The plastic deformation of ductile beams is

*Corresponding author, Associate Professor, Ph.D., E-mail: mdaniel@unina.it
[a] Ph.D. Student, E-mail: dcassiano@student.dec.uc.pt
[b] Assistant Professor, E-mail: crebelo@dec.uc.pt
[c] Professor, Ph.D., E-mail: landolfo@unina.it
[d] Professor, Ph.D., E-mail: luisss@dec.uc.pt

http://www.techno-press.org/?journal=scs&subpage=6 ISSN: 1229-9367 (Print), 1598-6233 (Online)

characterized by strain hardening, which is responsible for the development of bending moments larger than the plastic bending strength (D'Aniello *et al*. 2012, 2014, 2015, Della Corte *et al*. 2013, Güneyisi *et al*. 2013, 2014, Tenchini *et al*. 2014). Therefore, according to hierarchy criteria, non-dissipative elements (namely connections and columns) should be designed to resist the maximum bending moment experienced by the beams. Consequently this philosophy leads to frames with strong column/weak beam assemblies. On the contrary, low/medium rise steel moment resisting frame (MRF) structures designed for lateral wind actions only, are typically characterized by a weak column/strong beam typology. It is evident that these two design philosophies should influence differently the structural robustness in case of progressive collapse. El-Tawil *et al*. (2014) showed that imposing a ductile damage pattern is favourable since it increases the structural capacity against progressive collapse. However, the required level of detailing to improve the building robustness in case of column loss scenarios is still an open issue.

In recent years, a large number of studies have been carried out on structural robustness and the progressive collapse of structures, as well. Izzuddin *et al*. (2008) proposed a framework for evaluating robustness based on the computation of the system pseudo-static capacity. Pushdown analysis was also used in studies conducted by Lu *et al*. (2012) concluding that failure modes were correctly determined using pushdown analysis and that robustness can be quantified using the residual strength ratio. The loss of stability induced progressive collapse modes were studied by Gerasimidis *et al*. (2014). Numerical studies by Dinu *et al*. (2015), Khandelwal *et al*. (2008) and Hayes *et al*. (2005) showed that frames designed using seismic design provisions may improve robustness and Gerasimidis and Baniotopoulos (2015) evaluated the effectiveness of different collapse mitigation strategies. Khandelwal *et al*. (2008) also concluded that layout and system strength significantly influence robustness. Jahromi (2009) verified that the response under column loss is dominated by a single mode. The importance of the three-dimensional effects on dynamic response was addressed by Alashker *et al*. (2011) concluding that 2D modelling does not necessarily lead to conservative results and that 3D analysis is required to rigorously investigate robustness. The influence of column loss action rise time was investigated by Comeliau *et al*. (2010) and a method for quantifying the maximum dynamic displacement for planar frames was proposed. An analytical method based on critical ductility curves was proposed by Gerasimidis (2014) to predict the collapse mechanism for the case of a corner column loss. A study by Fu (2010) showed that for many beams designed according current design practice, no plasticity is developed and catenary effect is not developed. A parametric study by Grecea *et al*. (2004) highlighted the performance differences for different types of moment frames subjected to seismic motion. The influence of different types of connections on robustness was investigated by Kim and Kim (2009). Formisano and Mazzolani (2010, 2012) and Formisano *et al*. (2015) highlighted that both full strength and rigid connections allow achieving satisfactory robustness levels, whereas semi-rigid ones exhibit inferior performance although providing adequate behaviour when they are full strength. Studies by Ruth *et al*. (2006) showed that a dynamic increase factor (DIF) of 2.0 is overly conservative and that more economic design can be achieved. Starossek and Haberland (2008) addressed the subject of robustness measures.

The effectiveness of seismic detailing according to EN 1998-1 (CEN 2004) on improving structural robustness is still under discussion, and although there is some consensus (Hayes *et al*. 2005, Khandelwal *et al*. 2008, Kim and Kim 2009) that seismic detailing might be beneficial, quantification of this effect is still required. Adopting capacity design principles alone as a prescriptive measure for improving robustness presents shortcomings similar to prescriptions given by other codes (e.g., EN 1991-1-7 (CEN 2006), UFC 2009 (USDoD 2009) for addressing robustness, such as the "Tie Force Method" or the "Key Element Design", which aim at assuring minimum levels of structural continuity and robustness. These considerations motivated the study presented in this paper, which is aimed at quantifying structural robustness of steel MRFs under column loss scenarios and at assessing the efficacy of seismic detailing on arresting a progressive collapse under different column loss scenarios. To this end, a numerical parametric study based on both nonlinear static and dynamic analysis was carried out on a set of reference frames, varying both mechanical and geometrical parameters and the relevant main outcomes are described and discussed hereinafter.

2. Framework of the study

2.1 Investigated parameters

A set of 48 different buildings equipped with MRFs was designed varying the following parameters: number of storeys, interstorey height, span, bay configuration and design lateral loads (i.e., wind or earthquake). These variables have been selected in order to cover a wide range of realistic structures. The list of investigated parameters and corresponding values is presented in Table 1.

As shown in Fig. 1(a), each structure presents two MRFs per direction, while the remaining parts are designed to resist gravity loads only. Since the influence of joint detailing is out of the scope of this study, the beam-to-column joints of the MRFs were assumed as full strength rigid connections in all examined cases, whereas the joints in the secondary frame were modelled as perfectly pinned. An exception to these MRF layouts was considered for the 8-storey seismically designed structures with 10 m spans. Indeed, for those cases, all frames in both directions were designed to be moment resisting with full strength rigid primary beam-to-column connections

Table 1 Parametric variable definition

Parametric variable	Variable symbol	Values	Units
Number of storeys	N	{4; 8}	[-]
Interstorey height	H	{3; 4}	[m]
Bay span	S	{6; 10}	[m]
Bay layout configuration	T	{5×3; 4×4; 5×4}	[-]
Lateral load scenario	D	{Wind (W); Seismic+Wind (E)}	[-]
Column loss scenario	L	{Long façade (L); Short façade (S); Corner (C)}	[-]

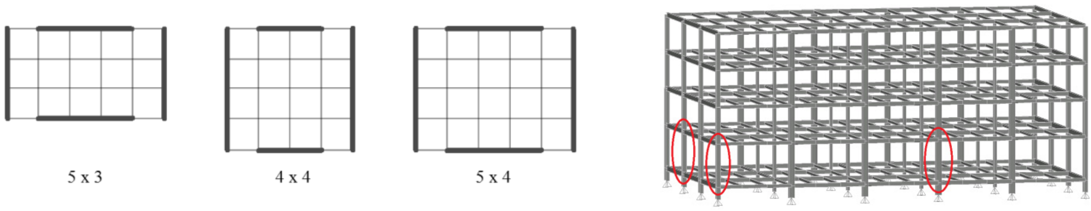

(a) Plan layouts (b) Column removal location scenarios

Fig. 1 Moment resisting frames

and cruciform cross sections for columns. The cruciform cross sections are symmetrical about the main axes and are built up by welding a pair of steel wide flange profiles. For each structure, as presented in Fig. 1(b), three column removal location scenarios were analysed: (i) internal column along the X direction façade (LL); (ii) internal column along the Y direction façade (LS); (iii) corner column (LC). The positions of column loss were defined in accordance with the UFC 2009 (USDoD 2009), considering in all cases that the section to be removed is located between the ground level and the first storey.

2.2 Design assumptions

The set of frames was designed according to Eurocodes. In particular, the design actions and relevant loading combinations are compliant to EN 1991-1-7 (CEN 2006), while the verification checks and the requirements for seismic design are in accordance with EN 1993-1-1 (CEN 2005) and EN 1998-1 (CEN 2004), respectively. S355 steel grade was assumed for all structural members except for two cases where S460 was adopted for columns (i.e., the 5×4 and 4×4 seismically designed structures with 8 storeys) in order to satisfy the strength requirements for N-M-V interaction at Ultimate Limit State. Horizontal in-plane bracings were assumed to guarantee a diaphragmatic behaviour of each floor, which was conceived in order to avoid any composite behaviour with all (both primary and secondary) beams (i.e., all steel solution).

Structures designed for the load scenario DE (see Table 1) were conceived to resist both gravity and seismic actions, according to capacity design principles required by EN 1998-1. These structures were subsequently verified against wind actions and redesigned whenever necessary, while maintaining compliance with the seismic design requirements (i.e., strong column – weak beam). Conversely, structures designed for the load scenario DW (see Table 1) were conceived to resist solely gravity and wind actions in order to satisfy all limit states according to EN1993-1-1. In this case, the dimensions of columns were directly obtained from elastic analysis and no hierarchy of resistance was considered, thus leading to strong beam-weak column frames.

Permanent structural loads were assumed equal to 1.7 kN/m^2 for all storeys and permanent non-structural loads of 1.2, 1.4 and 1.2 kN/m^2 were adopted for the ground floor, elevated storeys and roof, respectively. Live loads of 4.0, 3.0 and 0.4 kN/m^2 were adopted for the ground floor (commerce), elevated storeys (office) and roof, respectively. In addition, considering that the accidental action combination indicated in EN 1991-1-7 factors the wind action by 0, the only horizontal loading applied to the MRFs corresponds to the initial sway imperfection which is accounted for by a system of equivalent horizontal forces, as indicated in EN 1993-1-1. In terms of wind action, a basic wind velocity of 30 m/s was considered on a Type III terrain category, which is characteristic of suburban areas. In this case, moderate wind actions were selected given that designing for strong wind actions can provide MRF structures with levels of robustness which are not representative of most building structures in European urban areas. The seismic action was defined according to the EN 1998-1. Seismic actions types 1 and 2 were used, considering soil type C, importance class II, ductility class DCH, behaviour factor q = 6.5 and a peak ground acceleration of 0.25 g.

On the basis of the above described actions, in order to highlight the design overstrength of the frame that influences the structural robustness, the margins of safety Ω at both serviceability limit state (SLS) and ultimate limit state (ULS) were also calculated for all examined frames as follows

$$\Omega = \frac{R - E}{E} \tag{1}$$

Table 2 Average margin of safety factors Ω for moment resisting and secondary gravity frame elements

Moment resisting frame							Secondary gravity frame				
N	S	D	Ω_{SLS}	$\Omega_{ULS,BEAM}$	$\Omega_{ULS,COLUMN}$	$\Omega_{ULS,JOINT}$	Element	S	Ω_{SLS}	Ω_{ULS}	$\Omega_{ULS,JOINT}$
-	m	-	-	-	-	-	-	m	-	-	
4	6	W	0.08	1.51	1.03	0.22	Primary	6	0.88	0.23	0.19
		E	0.15	0.81	0.29	0.39	Internal beam	10	0.32	0.19	0.12
	10	W	0.14	0.13	0.71	0.24	Primary	6	0.76	0.29	0.28
		E	0.07	0.17	0.06	0.41	Perimeter beam	10	0.24	0.35	0.11
8	6	W	0.05	2.08	0.51	0.26	Secondary	6	7.82	0.22	0.23
		E	0.19	1.10	0.12	0.43	Internal beam	10	14.00	0.22	0.14
	10	W	0.14	1.32	0.07	0.27	Secondary	6	6.89	0.20	0.20
		E	0.18	0.61	0.05	0.45	Perimeter beam	10	11.50	0.30	0.13
							Internal	6	-	0.22	-
							Column	10	-	0.04	-

where R is alternatively the displacement limit at SLS or the design factored strength at ULS of structural members, while E is the maximum effect induced by design actions, respectively at either SLS or ULS.

Table 2 summarizes the average margin of safety factors for the analysed frames. As it can be recognized, the beams of MRFs designed against either DW or DE lateral load scenarios are characterized by the higher Ω_{ULS} values, which is due to the need to satisfy drift limitation and overall stability requirements. On the contrary, the beams of gravity load resisting frames are characterized by the lower Ω_{ULS} values, because their design was mainly influenced by lateral torsional buckling verification checks for the constructional phase condition. This issue also explains large Ω_{SLS} values. The columns of MRFs designed under DE scenario are characterized by low Ω_{ULS} values, because of capacity design requirements. Also the gravity resisting columns are characterized by small safety margin. Conversely, the columns belonging to MRFs designed under DW scenario have the larger Ω_{ULS} values, owing to the need to control lateral drifts. Finally, full strength joints (more details are given in Section 3.1) were assumed for MRFs, characterized by safety margins ranging from 0.22 to 0.45 (N.B. lower for wind design frames and larger for seismic resisting structures). Pinned joints (see Section 3.1), were considered for gravity load frames, with by safety margins ranging from 0.11 to 0.28, being the lower values for long span.

2.3 Monitored parameters

The Alternative Load-path Method (ALM) is widely used to evaluate the robustness of steel frames (GSA 2003, USDoD 2005, 2009) and is generally combined with a threat independent approach, characterized by instantaneous column loss, to evaluate the capacity of structures to internally redistribute loads and to arrest a progressive collapse. However, ALM does not provide further information about the reserve capacity of the structural system (Khandelwal *et al*. 2008) and, consequently, does not allow distinguishing between structures with large and negligible reserve capacities. Hence, it is essential to adopt measures of robustness that provide a measurement of the system's sensitivity to localized failure. As highlighted by Starossek and

Haberland (2008), none among the methods used to assess robustness can be considered as the most effective or suitable in all cases, since different types of collapse mechanisms can be better described by using specific measures.

Robustness measures may be subdivided into two groups, namely local and global robustness measures. The former type evaluates robustness locally through demand-to-capacity ratios, whereas the latter type expresses global robustness through a ratio between the load capacity of the damaged structure and the nominal gravity loads (El-Tawil *et al*. 2014). Several approaches to measuring robustness have been proposed by different authors, such as the risk based robustness index (Baker *et al*. 2008), the energy based partial pushdown analysis procedure (Xu and Ellingwood 2011) or deterministic robustness indexes (Lalani and Shuttleworth 1990). In this study, a deterministic global robustness measure was adopted, namely the Residual Strength Ratio (*RSR*) of the system evaluated as follows

$$RSR = \frac{F_{u,damaged}}{F_{dyn,damaged}} \tag{2}$$

where ($F_{u,damaged}$) is the ultimate capacity of the structural system in the damaged configuration and ($F_{dyn,damaged}$) is the equivalent dynamically amplified force for which the system reaches equilibrium in the damaged state, which is obtained as shown in Fig. 2(b).

It should be noted that *RSR* given by Eq. (2) differs from the index used by Lalani and Shuttleworth (1990), because these Authors assumed their redundancy index as the ratio between collapse and design loads.

The capacity of a system to respond to a column loss action in the plastic range by taking advantage of global ductility can be expressed by the Dynamic Load Factor (*DLF*) which accounts for inertial and nonlinear effects (USDoD 2009) and is given by the following ratio

$$DLF = \frac{F_{dyn,damaged}}{F_{stat}} \tag{3}$$

where ($F_{dyn,damaged}$) is the equivalent dynamically amplified force for which the system reaches equilibrium in the damaged state, and (F_{stat}) is the value of the static gravity loads on the resisting element prior to notional removal.

2.4 Analysis methodology

2.4.1 Pushdown analysis

For pushdown analysis, both material and geometrical nonlinearities were accounted for. In addition, the internal force distribution in the element to be removed was initially determined in accordance with the accidental load combination given in the EN 1991-1-7, and the column segment was replaced by the equivalent reactions. Subsequently, increasing vertical displacements were imposed to the node to which equivalent column reaction forces were applied, hence generating the vertical force-displacement pushdown curve. The procedure adopted to assess structural robustness by means of pushdown analyses was the energy balance method proposed by Izzuddin *et al*. (2008). This methodology allows computing the system pseudo-static capacity by imposing a zero kinetic energy condition, and consists of three stages: (i) Determination of the nonlinear static response of the structure under gravitational loading; (ii) Simplified dynamic assessment through energy balance to establish the maximum dynamic response; (iii) Ductility

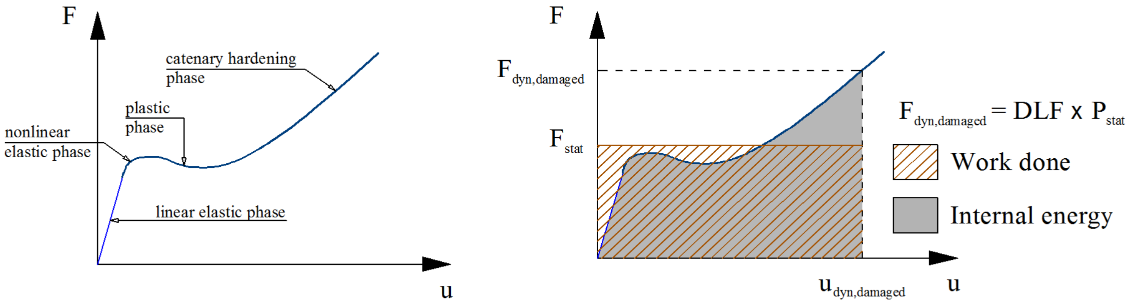

(a) Structural behavioural phases (b) System internal energy and work done

Fig. 2 Typical nonlinear static structural response according to Izzudin *et al.* (2008)

assessment of the connections. The computation of the response implicitly assumes that the directly affected zone behaves as a Single Degree of Freedom (SDOF) system, which is considered a reasonable hypothesis for robustness assessment purposes (Jahromi 2009).

The structural response under column loss is characterized by an initial linear elastic phase, followed by a nonlinear phase due to geometric and material nonlinearity, and finally by an eventual hardening phase due to catenary effect, or alternatively by a softening phase due to buckling or failure of structural elements. The typical nonlinear static structural response is presented in Fig. 2.

The application of the energy balance method requires the computation of the external work done (which is equal to the axial force in the column prior to removal times the total vertical displacement at each step of the pushdown analysis) and the computation of the internal energy (which is given by integral of the Force-Displacement system response curve) for all vertical displacement values. The external work done W_{ext} and the internal energy W_{int} at the vertical pushdown displacement u_i are given by

$$W_{ext} = F_{stat} \times u_i \tag{4}$$

$$W_{\text{int}} = \int_0^{u_i} F(u) \times du \tag{5}$$

Equilibrium in the damaged configuration is achieved by imposing the zero kinetic energy condition, which is obtained when the energy balance is equal to zero, i.e., when the work done is equal to the internal energy

$$\Delta W = W_{ext} - W_{\text{int}} = 0 \tag{6}$$

$$F_{stat} \times u_i - \int_0^{u_i} F(u) \times du = 0 \tag{7}$$

The displacement value u_i for which the condition indicated in Eq. (7) is verified corresponds to the equivalent dynamic displacement at equilibrium $u_{dyn,damaged}$ defined in Fig. 2(b). For the cases in which the energy balance is not obtained, the zero kinetic energy condition is therefore not reached and global structural collapse occurs.

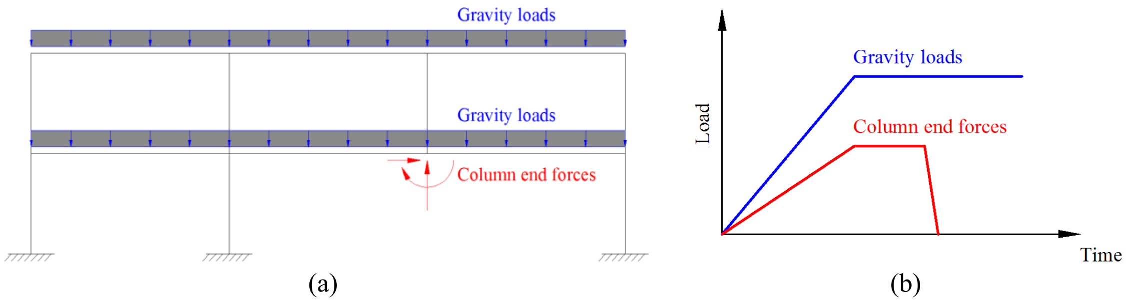

Fig. 3 Gravity and column loss load time history application for NDA

2.4.2 Nonlinear dynamic analysis

For the nonlinear dynamic analysis (NDA), a threat independent approach was adopted by considering a pseudo-instantaneous column removal. The load combination used for pushdown analysis was also considered for NDA, namely the accidental load combination described in EN 1991-1-7. In the first step, the equivalent reaction forces at the column end for the accidental load combination were determined. Subsequently, the gravity and the column equivalent reaction loads were applied according to a ramp function as shown in Fig. 3. GSA guidelines (GSA 2003) recommend assuming a time interval t_r for the decreasing ramp function equal to or smaller than 1/10 of the natural vibration period of the structure. In order to verify the applicability of the recommended t_r value for the threat-independent analysis, a sensitivity study on column removal action rise time was preliminarily carried out, which concluded that a rise time $t_r = 0.01$s was suitable to perform the analyses.

The NDAs were performed accounting for both geometrical and material nonlinearities, and using the Hilber-Hughes-Taylor alpha method (CSI 2009) with an alpha coefficient equal to 0 and a time step of 0.01s for the direct integration method. In order to avoid overdamping, Rayleigh tangent damping ratio $\zeta = 2\%$ was considered for a frequency of 1 Hz and for the structure's natural frequency of vibration in the damaged configuration. The applicability of the assumed value for the damping ratio was also verified by performing a sensitivity analysis for the examined column removal scenarios.

The type of vibration mode after column loss (i.e., either multiple or single vibration mode dominated behaviour) was also extracted from NDA response curves, and the joint rotation demands at the equilibrium condition in the damaged configuration were determined, as well.

3. Numerical analysis

3.1 Modelling assumptions

The numerical models of the structures were developed using the software SAP 2000 (CSI 2009). Geometric nonlinearities were taken into account according to the P-Delta formulation with large displacements (CSI 2009). Material nonlinearity was modelled through a lumped plasticity formulation. The plastic hinge response curves and the relevant acceptance criteria were derived according to FEMA 356 (ASCE 2000). Although the parameters provided by FEMA 356 refer to cyclic loading and despite the fact that modelling criteria given by UFC 2013 (USDoD 2013) are specifically derived for pushdown analysis, the response of the examined beam-to-column joint is

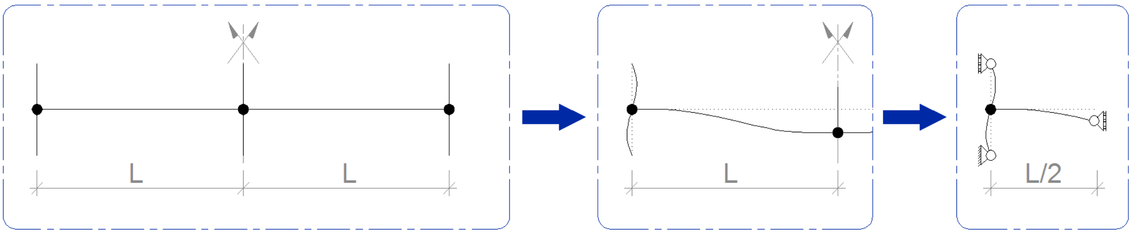

Fig. 4 Substructure selection for joint modelling validation

better described by the relationship provided by FEMA 356 (see Fig. 5(a)). This is due to the fact that UFC 2013 does not provide modelling criteria specifically devoted to simulate the behaviour of full strength bolted moment connections that are the typology considered within this study.

The beams of both MRF and gravity resisting spans are all-steel members, because no composite action was considered with the floor that is simply supported by the steel girders. Anyway, the diaphragmatic behaviour is guaranteed by the presence of in-plane bracing at floor level. The beam-to-column joints of the MRF beams were modelled as full-strength rigid joints, while the gravity designed beams were considered as perfectly pinned at both ends. Since the behaviour of the joints of both MRF and secondary frames plays a key role in determining the frame robustness, the validity and consistency of the above described modelling assumptions were verified against finite element analysis (FEA) of beam-to-column joint sub-assemblies, which were selected according to the sub-structuring procedure depicted in Fig. 4.

For what concerns the joint typologies, bolted joints with extended endplate, rib stiffeners and additional column web panel configurations were considered for MRF, while flush endplate beam-to-column joints were assumed for the secondary structure, since both joint configurations are widely used in European practice. The joints have been designed according to the EN 1993 (CEN 2005) and EN 1998 (CEN 2004) for all beam-column assemblies of the frames reported in Table 1. Hereinafter, for briefness sake, the results from FEAs are described and commented for the most representative joints. In particular, the assembly consisting of an IPE 600 beam and an HEB 500 column was found to be representative of the MRF, because it is the one characterized by the deeper beam, thus potentially developing the larger catenary action on the connection. For the secondary structure, the results obtained for a flush endplate joint with an IPE 220 beam connected to an HEB 500 column are shown, because this joint is characterized by the weaker connection among those of all gravity resisting joint assemblies.

The finite element models were developed using Abaqus ver. 6.13 (Dassault 2013). The finite element type C3D8I (an 8-node linear brick, incompatible mode) was adopted for steel beams, columns and high strength bolts. This element was selected because it can effectively avoid shear-locking phenomenon (comparing with element C3D8R), which could significantly affect the initial stiffness of connection. Steel yielding was modelled by means of the von Mises yield criteria and plastic hardening was represented using a nonlinear kinematic and isotropic hardening. The external restraints were simulated by slaving to reference points (RP) the nodes belonging to the end cross sections of the beam and column. Contact phenomena were modelled considering the general contact algorithm using a Coulomb friction model. A penalty friction formulation was adopted and a friction coefficient of 0.3 was adopted.

Considering that the MRF beam-to-column joints are subjected to important catenary forces following column loss actions, two MRF joint configurations were analysed, namely a joint with standard detailing (T1) and a joint with improved detailing (T2) consisting of an additional bolt row in the middle of end plate (namely in the horizontal axis of symmetry). The moment - chord rotation response curves for MRF joint types T1 and T2 are presented in Fig. 5(a), and compared with the plastic hinge response according to FEMA 356, UFC 2013 and the beam plastic bending moment $M_{pl,beam}$, the latter computed in accordance with the EN 1998-1 (CEN 2004). In addition, the joint deformed shapes at an imposed chord rotation equal to 100 mrad are shown in Fig. 5(b).

As it can be noticed, both T1 and T2 joints are full strength and exhibit satisfactory response under column loss action, with bending strength being higher than the beam plastic capacity $M_{pl,beam}$ even at very large rotations. The improved detailing of T2 has a beneficial effect under column loss actions, especially for chord rotation values higher than 100 mrad. The adopted FEMA 356 compliant response curve for plastic hinges shows a good agreement with the response of the T1 type joint (with standard detailing that is the type assumed for the examined structures), thus validating the adopted assumptions for MRF joints. The joint type T2 is out of the scope of this numerical study on building frames but it has been considered as a viable solution to improve joint performance if very large rotation demands are expected (Tartaglia *et al*. 2016).

Fig. 6 shows the comparison between the SAP model axial force-chord rotation response curve with that obtained from FEA of the flush endplate joint. As it can be observed, the adopted model adequately reproduces the catenary action developed in the joint under column loss action, thus

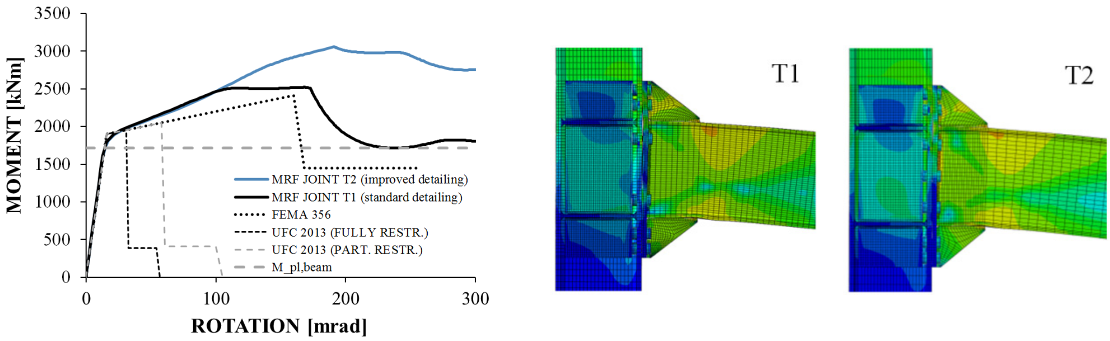

(a) Moment – chord rotation response (b) Deformed shapes (chord rotation = 100 mrad)

Fig. 5 MRF joints under column loss action

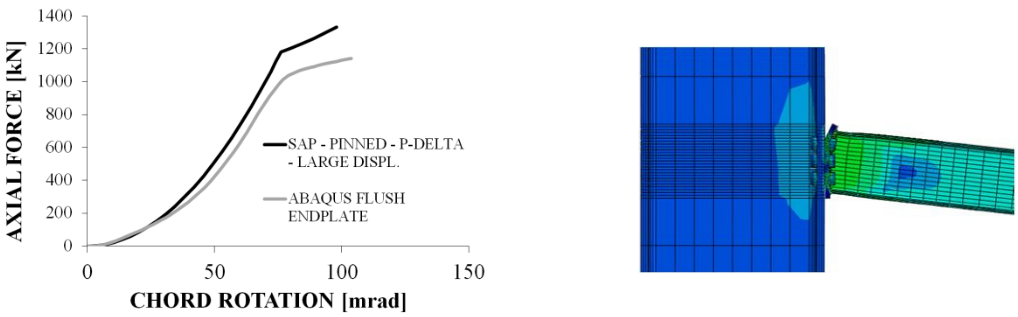

(a) Axial force – chord rotation response (b) Deformed shape (chord rotation = 100 mrad)

Fig. 6 Gravity load resisting joint under column loss action allowing deeming the joint response of the secondary beams sufficiently accurate for simulation.

3.2 Results from pushdown analysis

The overall response curves obtained from pushdown analyses are plotted in Fig. 7 for the examined column loss scenarios (e.g., long façade, short façade and corner, respectively).

The comparison of pushdown results allowed the identification of three types of global failure mechanism, namely: (i) Type I - characterized by high ductility due to the distribution of plasticity throughout the beam elements of the directly affected zone; (ii) Type II - characterized by poor ductility and typically conditioned by brittle column failure between the ground floor and the first storey; (iii) Type III - semi-ductile and generally characterized either by column failure in the segment between the last elevated storey and the roof or by simultaneous failure in beam and column members. In terms of force-displacement response, Type I failure mode develops significant plasticity and achieves high ductility with large ultimate displacements; Type II failure

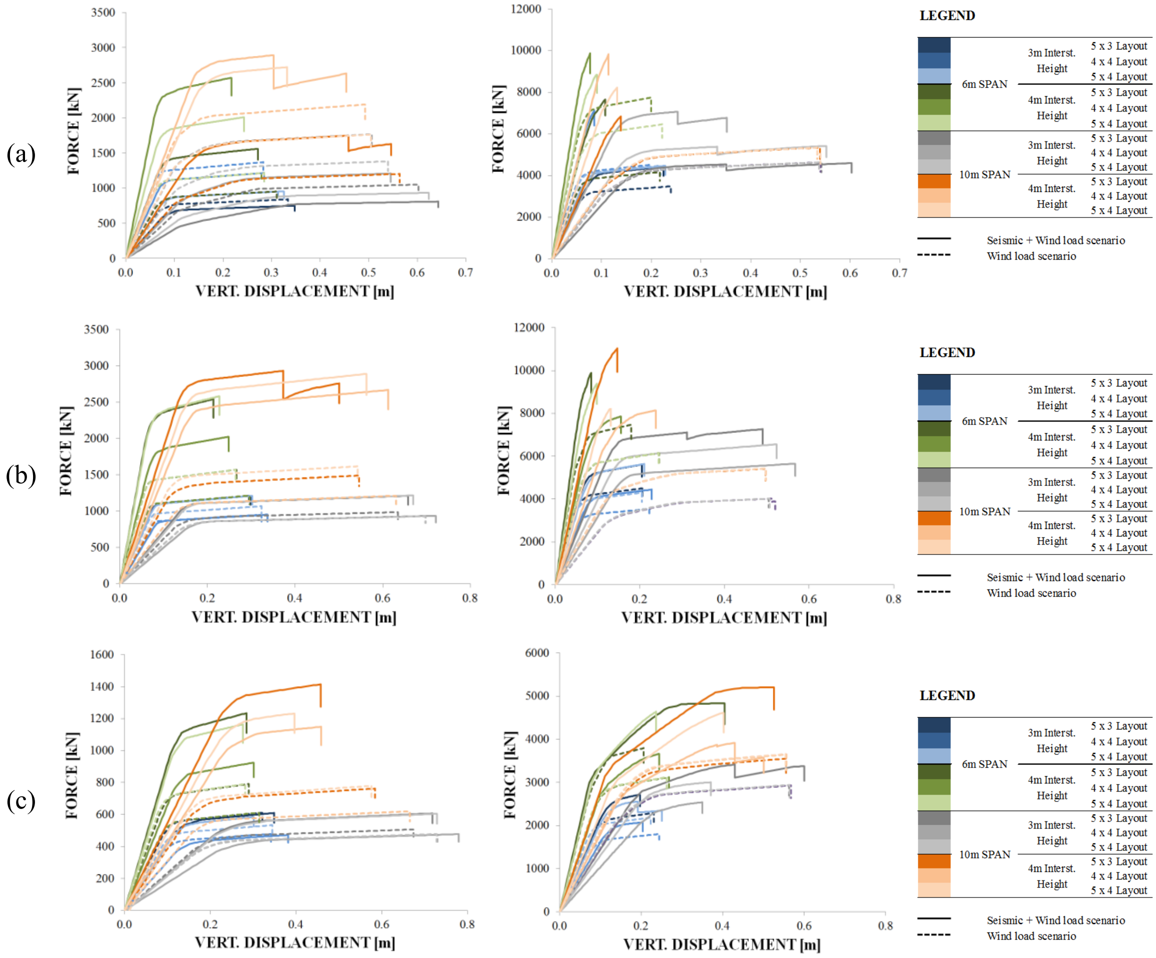

4 storey structures 8 storey structures

Fig. 7 Pushdown curves for column removal in (a) long façade; (b) short façade; and (c) corner mode presents linear elastic behaviour followed by sudden brittle failure associated to reduced ultimate displacements; frames with Type III failure develop an intermediate mechanism characterized by an initial plastic response followed by an early drop of resistance, after which a small plastic plateau is generally observed followed by full collapse at moderate ultimate displacements. The distribution of occurrence per failure type was analysed and results showed that the ductile Type I failure was observed for 94% and 61% of 4-storey and 8-storey buildings, respectively, while the corresponding occurrence of Type II failure was the 1% and 31%, highlighting that 8-storey structures are more susceptible to less ductile collapse modes. For what concerns the influence of the lateral load design scenario, all seismically designed structures presented ductile failure (i.e., mode Type I), whereas for the strong beam – weak column structures, 44% of failures were semi-ductile (i.e., mode Type III), or brittle (i.e., mode Type II).

3.2.1 Residual strength ratio

The minimum acceptable *RSR* value for a structure is 1.0, which occurs when the equivalent dynamically amplified force for which the system reaches equilibrium in the damaged state $F_{dyn,damaged}$ is equal to the ultimate capacity of the structural system in the damaged configuration $F_{u,damaged}$ (see Eq. (2)). For cases in which the internal energy did not balance the work done, equilibrium was not reached and the *RSR* was taken as 0, indicating zero residual strength.

The *RSR* values for the 4 storey structures are presented in Fig. 8 for the 6 m span and 10 m span structures. The analyses showed that the long span structures exhibit the lower values of *RSR*, with failure occurring in several cases, whereas no failures were observed for short span structures. These results are mainly due to two aspects: the longer is the span, the larger is the resultant of vertical loads requiring redistribution, and the larger is the demand on beam-to-column assemblies in terms of bending and catenary actions, as well.

As a general remark, all examined 4-storey structures characterized by deeper beams develop Type I overall failure mode, which mobilises the Vierendeel mechanism in the alternative load path, thus experiencing high ductility. Considering that wind designed structures present beams with larger cross sections dimensions, their capacity is comparatively higher than that of the seismically designed structures. Higher values of *RSR* were also observed for buildings with taller interstorey height. Once again, this result depends on the dimensions of girder cross section, which are deeper for taller buildings due to the need to limit storey drifts.

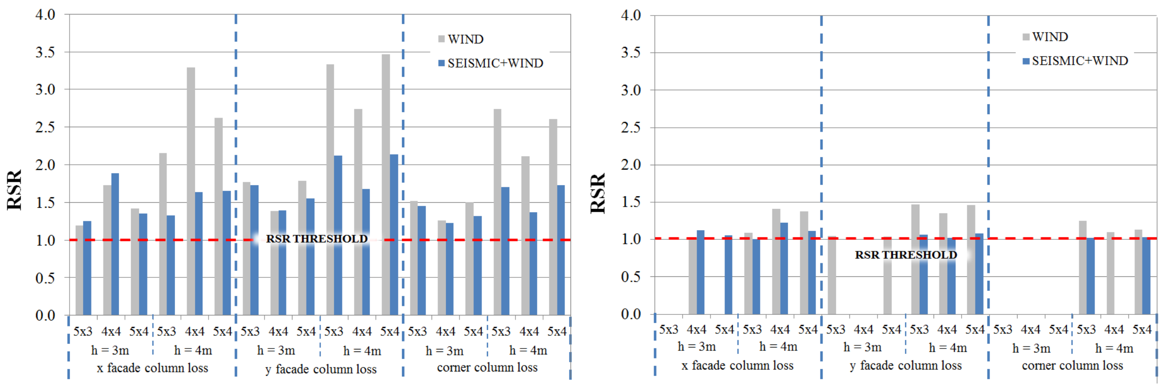

(a) 6 m span structures (b) 10 m span structures

Fig. 8 Residual Strength Ratios - 4 storey frames

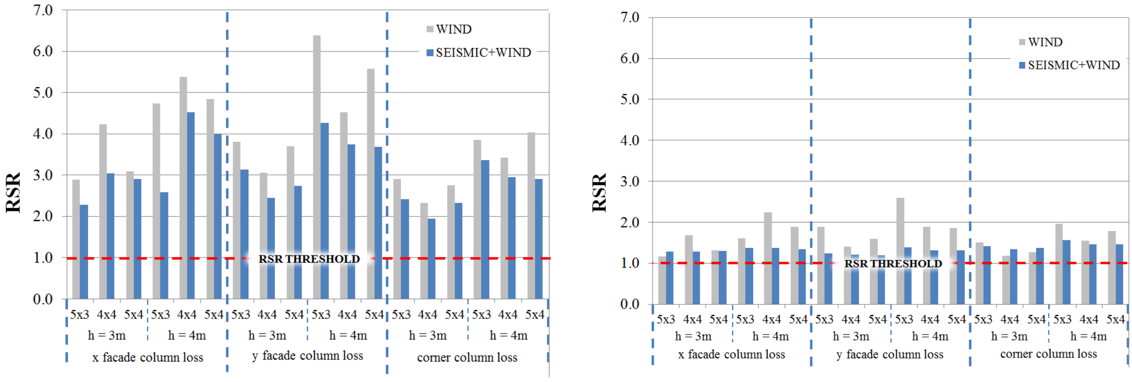

(a) 6 m span structures (b) 10 m span structures

Fig. 9 Residual Strength Ratios – 8 storey frames

The *RSR* values for the 8-storey structures are presented in Fig. 9. Similarly to 4-storey frames, also in this case the ratios for the 10 m span frames are close to 1.0, whereas 6 m span frames provide larger robustness levels.

For both 4- and 8-storey frames, numerical results highlighted that the position of column loss scenario may influence *RSR*, especially for the cases of corner column loss that are characterized by lower robustness due to limited redistribution capacity. In addition, bay layout plays an important role. Indeed, structures with planar MRFs composed of few heavy elements (e.g., 4×4 bay layout in the *x*-*z* plan) are characterized by higher robustness levels. The number of spans belonging to the directly affected zone appreciably influences the frame robustness, as well.

In order to highlight the influence of seismic detailing on frame robustness, the *RSR* of seismic designed MRFs (i.e., weak beam – strong column) are compared to those of wind designed structures (i.e., strong beam – weak column) as depicted in Fig. 10. The *RSR* distribution outlines that the wind designed structures generally provide higher robustness, especially for the case of 8-storey frames.

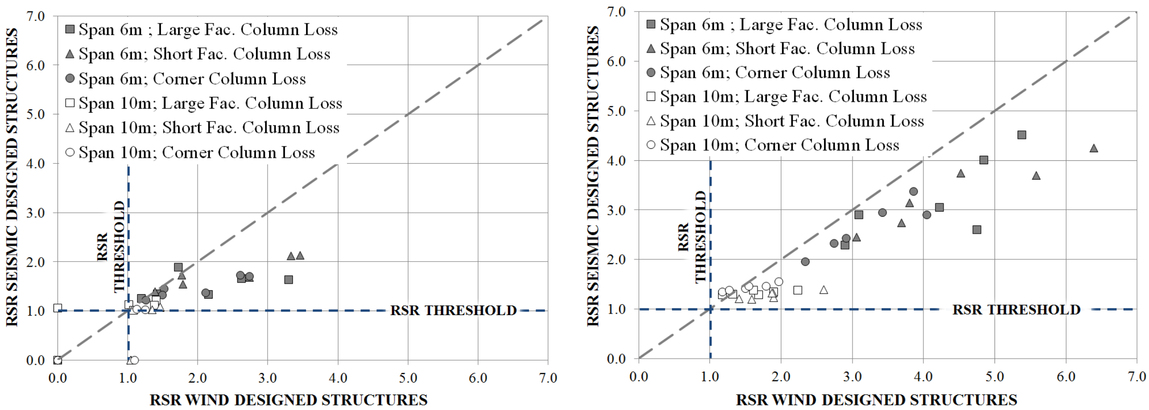

(a) 4-storey frames (b) 8-storey frames

Fig. 10 Residual Strength Ratio comparison

It is interesting to observe that seismic designed structures present smaller scatter of *RSR* than wind designed frames. This feature depends on the occurrence of failure modes. Indeed, all EC8 compliant MRFs are characterized by a Type I mechanism, while the set of wind design MRFs experienced all three types of failure modes. However, although seismic detailing provisions enforced a global ductile failure mode in all cases, it is not possible to find a direct correlation between adopting seismic provisions and enhanced robustness.

3.2.2 Dynamic load factors

The *DLFs* were computed according to Eq. (3) in order to estimate the capacity of structures to exploit ductility in arresting a progressive collapse. In order to clarify the results described hereinafter, it should be noted that a *DLF* equal to 2.0 represents a purely elastic response, and a value equal to 1.0 corresponds to a theoretically rigid-plastic response, while a zero value corresponds to structural collapse. In non-collapsed cases, *DLFs* range from 1.0 to 2.0.

Fig. 11 reports the distribution of *DLF* for 6 m and 10 m span structures, highlighting the role of the main investigated variables, like the column loss scenarios, the type of design lateral load and the number of storeys. As it can be observed, numerical results show that the majority of the 6 m span structures respond to column loss in the elastic domain (i.e., *DLF* = 2.0) and are capable of arresting the progressive collapse, as indicated by the absence of collapsed structures (i.e., *DLF* = 0.0). Only some of the 6 m span 4-storeys frames exhibit *DLF* slightly below 2.0, whereas for the 8-storey structures, all frames are in the elastic range, thus confirming the beneficial role of a large number of resisting elements above the zone directly affected by column loss. Fig. 11(a) also shows that frames’ lateral load design scenario for 6 m span frames does not influence *DLF*. The feature that short span frames essentially remain elastic implies that no permanent damage/deformation is sustained by the structure out of the parts directly affected by the column loss. In this sense, notwithstanding eventual localized damage (i.e., induced by the event which triggers the loss of column resistance), the required repairing interventions on the damaged frame are limited and can be made with reduced economical cost, since it mainly involves restoring the frame to its original position and replacing the damaged column segment.

The results for long (i.e., 10 m) span frames are reported in Fig. 11(b) and clearly show that several cases require the exploitation of frame ductility to arrest the collapse. Differently from the

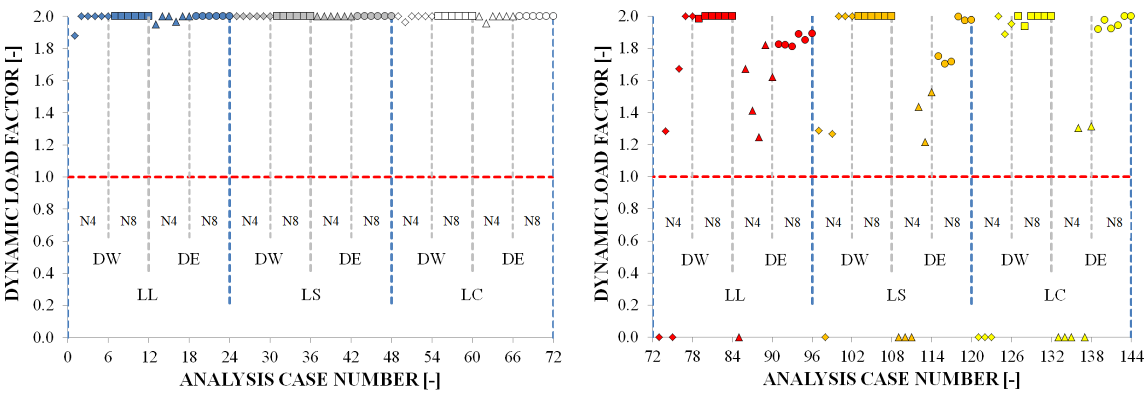

(a) 6 m span frames (b) 10 m span frames

Fig. 11 Dynamic Load Factor values by column removal scenario (LL, LS, LC), lateral load design scenario (DW, DE) and number of storeys (N4, N8) short span structures, for several cases, *DLFs* range between 1.0 and 2.0. As observed for *RSR* (see Section 3.2.1) the reason explaining the differences in performance between the 10 m span frames and the 6 m span ones can be found in the larger resultant of vertical loads requiring redistribution, which corresponds to larger demand on beam-to-column assemblies. Indeed, the examined long span frames considering column removal at building corner (namely with the smaller tributary area in the directly affected zone) are characterized by better performance with a pseudo-elastic response (*DLF* ≈ 1.9-2.0). It is also interesting to note that, differently from the previous set of buildings, seismic design criteria appreciably influences the performance of long span structures, which exhibit a larger capability to develop favourable plastic mechanism than the corresponding wind designed frames. Regarding the number of storeys, consistently with the results obtained for 6 m span buildings, also for this set of frames, the 8-storey MRFs show the better performance. In particular, *DLF* values are close to 2.0 for all wind designed structures, while ranging from 1.7 to 2.0 for seismic designed frames.

These results indicate that short span frames tend to remain elastic after the column loss, whichever design criteria is taken into account, whereas long span frames can require the development of plastic internal distribution to arrest progressive collapse. Therefore, the obtained results indicate that assuming for all cases a *DLF* equal to 2.0 (as suggested in GSA 2003) could be excessively conservative.

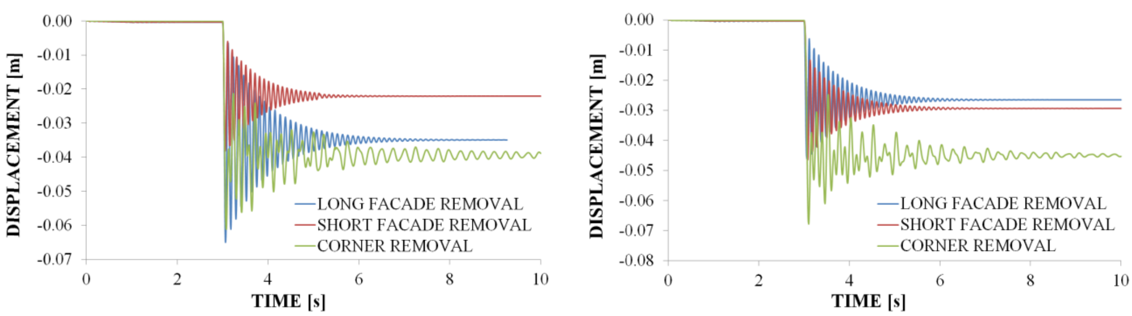

(a) 5×3 bay layout (b) 4×4 bay layout

Fig. 12 Time history response of the N4-H3-S6-DE frame under different column loss scenarios

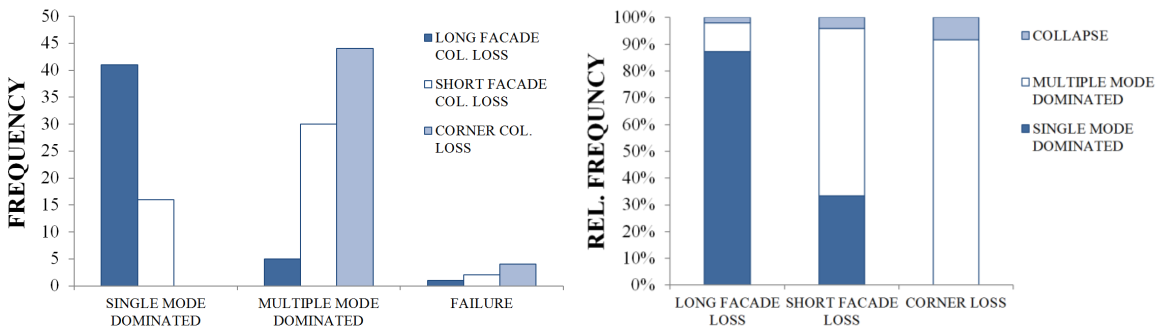

(a) By response type (b) By column loss scenario

Fig. 13 Column loss structural response

3.3 Nonlinear dynamic analysis results

3.3.1 Displacement time-history under column loss

The nonlinear dynamic response to the three considered column loss scenarios is illustrated in Fig. 12 for the cases of the 4-storey seismically designed frames, with 3 m interstorey height and 6 m span (N4-H3-S6-DE), for the 5×3 and the 4×4 bay layout configurations.

As depicted in Fig. 13, the cases subjected to corner column removal experienced a response dominated by multiple vibration modes, consistent with a MDOF system vibrating in a non-resonant condition, whereas for the majority of cases exposed to façade removal, the response was consistent with that of a SDOF system. This different vibrational response is due to a particularity of the structures. Indeed, in all examined frames the corner columns belong to MRF in one direction and to secondary structural beams on the other, which translates into large stiffness variations, causing the response to be dominated by multiple vibration modes. It should also be highlighted that in several façade removal cases, the position of the removed column is offset from the centre of the facade and multiple-mode dominated responses occurred in some cases. However, most long façade removal cases resulted in single-mode dominated responses, which is due to the fact that the long façade MRFs are generally composed of elements with higher stiffness and resistance than those of the short façade, thus providing a stabilizing effect under column loss that enforces the structure to have a single-mode response.

3.3.2 Pushdown vs. nonlinear dynamic analysis

The influence of dynamic effects was quantified by comparing the maximum displacements obtained from combined pushdown/energy balance method to those given by NDA.

By grouping results by column removal scenario as shown in Table 3, it can be recognized that the cases for long façade column removal exhibit the smaller mean ratio, which is due to the dynamic response of those cases that is basically single-mode dominated, rendering the NDA results more similar to those obtained from pushdown analysis. On the contrary, for both short façade and corner removal cases, higher values of the $u_{dyn,damaged,Pushdown}/u_{dyn,damaged,NDA}$ ratios were obtained due to the multiple-mode dominated response. Considering all examined cases (i.e., non-collapsed structures only), the average ratio μ is equal to 1.21, and the standard deviation s is equal to 0.15, with a coefficient of variation CV = 12.1%.

It is worth highlighting that the pushdown analyses correctly predicted all failure modes that were recognized with NDA. However, given that NDAs led to smaller maximum dynamic displacement values, some structures that collapsed according to the nonlinear static procedure, instead did not according to the NDA. This occurred in six cases of 4-storey – 10 m span frames (namely: N4-H3-S10-T5×3-DG-LC, N4-H3-S10-T5×3-DE-LL, N4-H3-S10-T5×3-DE-LS, N4-

Table 3 Pushdown vs. NDA: maximum dynamic displacement ratios related to column loss scenario

Column removal location	$u_{dyn,damaged,Pushdown}$ / $u_{dyn,damaged,NDA}$		
	m	s	CV
[-]	[-]	[-]	[%]
Long facade	1.14	0.18	15.7
Short facade	1.22	0.10	8.3
Corner	1.27	0.11	8.7
Total (all cases)	1.21	0.15	12.1

H3-S10-T5×4-DG-LL, N4-H3-S10-T5×4-DG-LC, N4-H4-S10-T4×4-DE-LC), characterized by very low RSR values and for which small variations of maximum dynamic displacement are critical in averting collapse. This result points out the importance of explicitly considering the dynamic effects, especially for structures with intrinsically low robustness, such as low rise - large span frames.

3.3.3 Rotation demand at equilibrium

In order to assess the level of rotation required to arrest a progressive collapse, maximum total chord rotations at damaged state equilibrium were computed. For the investigated frames, the span of the MRF beams is equal to the span of the secondary beams. Hence, the rotation demand on secondary structure joints is equal to the rotation demand on MRF joints. The total rotation demands obtained from the NDAs are presented in Figs. 14 and 15 for the 4- and 8-storey frames, respectively.

Results show that the maximum rotation demands for 10 m span frames are significantly higher than for 6 m span ones. For the 4-storey frames, maximum values of 64.1 mrad and 17.4 mrad were obtained for the 10 m and 6 m span frames, respectively. Hence, rotation demand is approximately 3.7 times larger because long span frames resist collapse predominantly via catenary action. A similar pattern is observed for the 8-storey structures, although with a smaller

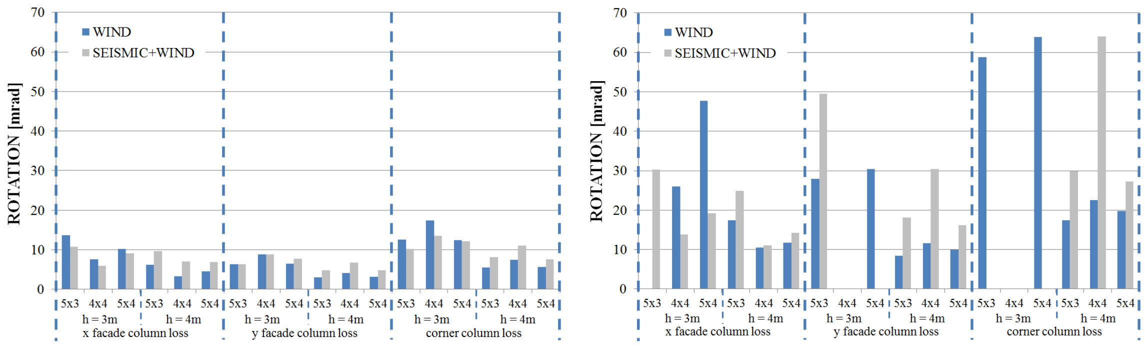

(a) 6 m span structures (b) 10 m span structures

Fig. 14 Total chord rotation demand for 4 storey structures

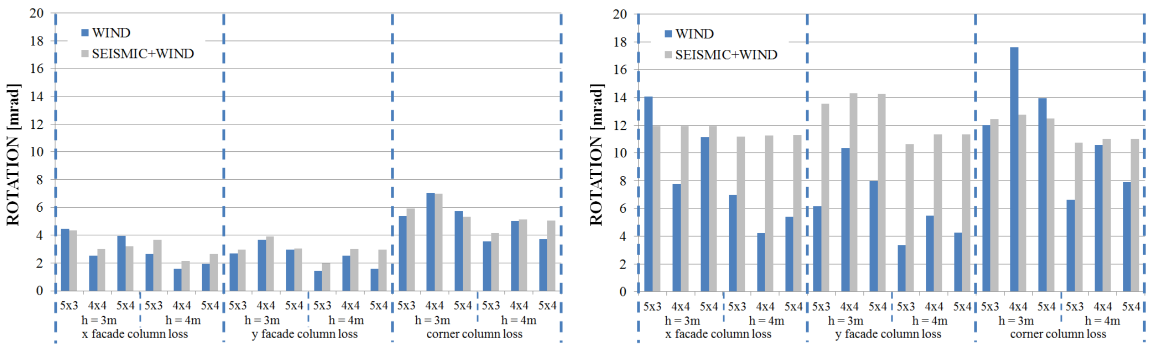

(a) 6 m span structures (b) 10 m span structures

Fig. 15 Total chord rotation demand for 8 storey structures difference due to the greater robustness of these structures. For the 8-storey structures the maximum rotation demand was 7.0 mrad for 6 m span and 17.6 mrad for 10 m span frames (approximately 2.5 times higher). These results highlight the high levels of joint rotational demand induced by column loss, for which joint detailing rules are not currently available in European codes. In the opinion of these Authors, similarly to what done for seismic resistant connections, there is a need for further studies in order to develop prequalification procedures for joints under column loss scenario.

4. Simplified prediction model for DLF

The numerical results discussed in the previous Sections show that *DLF* depends on the number of storeys (N) and on the lateral load design scenario (D). Therefore, a simplified method to estimate *DLF* values for MRF structures is proposed on the basis of the following equation

$$DLF = DLF_0 \cdot \delta_N \cdot \delta_D \tag{8}$$

The proposed expression factors the influence of the number of storeys (N) and of the lateral load design scenario (D) on the base value DLF_0, which corresponds to the *DLF* for a system responding in the elastic range ($DLF_0 = 2.0$). The influence of the number of storeys and of the design scenario is accounted for by the reduction factors d_N and d_D respectively. The reduction factor d_N was computed as the ratio between *DLF* values for 4 and 8 storey frames, whereas the reduction factor d_D was computed as the ratio between the *DLF* values for the seismic + wind designed (DE) and wind designed (DW) structures, as follows

$$\delta_N = DLF_{N4} / DLF_{N8} \tag{9}$$

$$\delta_D = DLF_{DE} / DLF_{DW} \tag{10}$$

being DLF_{N4} and DLF_{N8} the dynamic load factors for 4 and 8 storey frames, whereas DLF_{DE} and

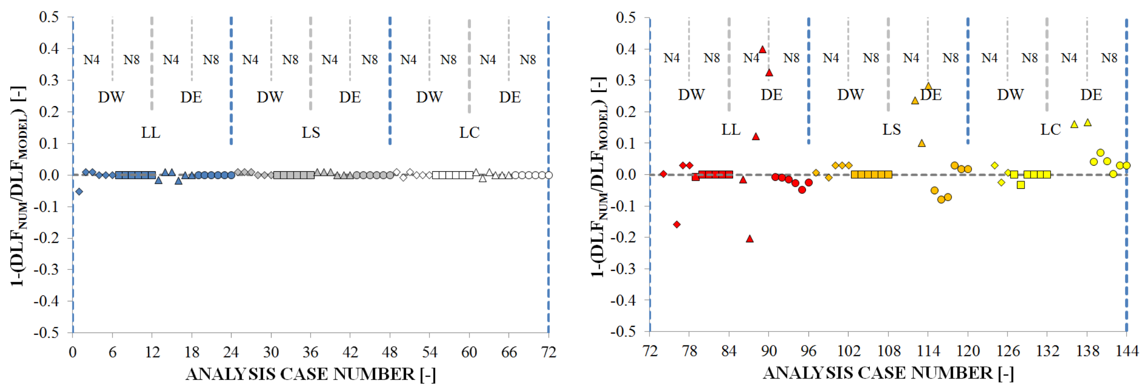

(a) 6 m span structures (b) 10 m span structures

Fig. 16 Comparison of the prediction accuracy of the proposed model and numerical results for *DLF*

Table 4 Proposed simplified prediction model for DLF

<table>
<tr><th>Bay span</th><th>Number of storeys</th><th>Lateral load design scenario</th><th>Interstorey height</th><th rowspan="2">DLF_0</th><th rowspan="2">d_N</th><th rowspan="2">d_D</th><th rowspan="2">DLF_{MODEL}</th><th rowspan="2">Improve detailing?</th></tr>
<tr><th>S</th><th>N</th><th>D</th><th>H</th></tr>
<tr><td>[m]</td><td>[-]</td><td>[-]</td><td>[m]</td><td>[-]</td><td>[-]</td><td>[-]</td><td>[-]</td><td>[-]</td></tr>
<tr><td rowspan="8">6</td><td rowspan="4">4</td><td rowspan="2">wind</td><td>3</td><td rowspan="8">2.00</td><td rowspan="8">1.00</td><td rowspan="8">1.00</td><td rowspan="8">2.00</td><td rowspan="8">N</td></tr>
<tr><td>4</td></tr>
<tr><td rowspan="2">seismic+wind</td><td>3</td></tr>
<tr><td>4</td></tr>
<tr><td rowspan="4">8</td><td rowspan="2">wind</td><td>3</td></tr>
<tr><td>4</td></tr>
<tr><td rowspan="2">seismic+wind</td><td>3</td></tr>
<tr><td>4</td></tr>
<tr><td rowspan="8">10</td><td rowspan="4">4</td><td rowspan="2">wind</td><td>3</td><td rowspan="8">2.00</td><td>0.64</td><td rowspan="2">1.00</td><td>1.28</td><td rowspan="4">Y</td></tr>
<tr><td>4</td><td>0.97</td><td>1.95</td></tr>
<tr><td rowspan="2">seismic+wind</td><td>3</td><td>0.85</td><td>1.00</td><td>1.70</td></tr>
<tr><td>4</td><td>0.74</td><td>0.74</td><td>1.09</td></tr>
<tr><td rowspan="4">8</td><td rowspan="2">wind</td><td>3</td><td rowspan="4">1.00</td><td rowspan="2">1.00</td><td rowspan="2">2.00</td><td rowspan="4">N</td></tr>
<tr><td>4</td></tr>
<tr><td rowspan="2">seismic+wind</td><td>3</td><td>0.92</td><td>1.84</td></tr>
<tr><td>4</td><td>0.97</td><td>1.95</td></tr>
</table>

DLF_{DW} are the values for the seismic + wind designed (DE) and wind designed (DW) structures, respectively. For 8 storey structures d_N is equal to 1, and for wind designed structures d_D is equal to 1. The coefficients of proposed prediction model are presented in Table 4. Fig. 16 depicts the accuracy of the proposed model with respect to the numerical results, which is generally satisfactory with little dispersion for most cases, predicting the dynamic amplification with reasonable accuracy (e.g., the scatter is smaller than 10% for 95% of examined cases). Indeed, only in 4 cases out of the 144 analysed cases the error was higher than 20%.

The points missing in Fig. 16 correspond to those cases where structures collapsed and therefore no *DLF* value could be computed. It should be noted that the larger dispersion was recognized for structures with low residual robustness, namely for seismically designed 4 storey – 10 m span frames, where the adoption of improved joint detailing (i.e., type T2 shown in Fig. 5 at Section 3.1) is recommended in order to significantly improve the joint capacity under catenary action. However, it is important to highlight that further studies are necessary to verify both effectiveness and generality of the proposed simplified model.

5. Conclusions

A parametric study based on pushdown and NDA was carried out to investigate the influence of seismic design criteria on the robustness of steel MRF structures for three column loss scenarios.

To this aim, 144 cases were examined, representative of two sets of 24 frames alternatively designed to resist either seismic action or wind action. The numerical results showed that structures designed according to the design requirements given by EN 1998-1 exhibit values of Residual Strength Ratio (*RSR*) lower than those obtained by frames designed according to EN1991 and EN1993, with lower dispersion as well. Consistently, the former structures are characterized by the same overall failure mode, while the latter showed three types of global collapse mechanisms providing different ductility levels and *RSR*. However, although seismic design criteria allow predicting and controlling the failure modes under column loss, seismic resistant steel MRF structures do not generally guarantee levels of robustness compatible with arresting progressive collapse. Provided that joints are able to resist to catenary actions, the analyses highlighted that both strength and stiffness of girders are crucial for improving robustness. Indeed, the better performance was provided by strong beam – weak column structures (i.e., non-seismic design frames), which are mostly characterized by elastic response after column loss, thus implying that these frames do not experience permanent deformation/damage, and enabling the feasibility to repair the frame. This satisfactory behaviour was also recognized for short span (i.e., 6 m) frames designed for seismic actions, which are the cases characterized by the larger beam-to-column stiffness ratios. Whichever the adopted design requirements, (either seismic or non-seismic) the results showed that structures with larger number of storeys experienced higher values of robustness, indicating that the number of elements mobilized through Vierendeel action is a key parameter in arresting a progressive collapse. On the contrary, the low *RSR* experienced by the 4-storey long span (i.e., 10 m) span frames highlights that this particular structural configuration needs improved detailing to avoid collapse subsequent to column loss. Feasible improved detailing may be achieved by adopting deeper girders than those strictly necessary to satisfy design code requirements, combined with improved MRF girder-to-column joint detailing. If bolted joints are used, performance can be improved by introducing supplementary bolt rows in the mid-height of the end-plate (i.e., in the beam's neutral axis) that are generally missing for joints designed to resist solely bending and shear. Moreover, the joints should be conceived to provide a rotation capacity larger than the demand that varies with structural configuration and column loss scenario. Indeed, low-rise and long span frames are characterized by the larger rotation demand. The average total rotation demands for joints are equal to 8.1 mrad and 26.2 mrad for the 4-storey 6 m and 10 m frames, respectively, while 3.7 mrad and 10.3 mrad are observed for 8-storey 6 m and 10 m frames, respectively. Since joint detailing rules for avoiding progressive collapse are not currently provided by European codes, further studies are necessary in this field. With this regard, in the opinion of the Authors, prequalification procedures should be introduced in order to develop adequate design rules for steel beam-to-column joints under column loss scenario.

The non-linear dynamic analyses have also enabled to identify two types response, namely single and multiple-mode dominated. All corner column removal cases showed multiple-mode response, whereas for the façade removal scenarios the response was mostly single-mode type. The average displacements obtained from NDAs are smaller than those given by pushdown analyses combined with the energy balance method, in the range between 14 to 27%, depending on the column removal scenario and failure mode. A simplified prediction model for the Dynamic Load Factor was also proposed, taking into account frame span, number of storeys and lateral load design scenario. The accuracy of the proposed model is satisfactory with scatter lower than 10% for 95% of the analysed cases. However, further study is necessary to verify its effectiveness and generality.

References

Alashker, Y., Honghao, L. and El-Tawil, S. (2011), "Approximations in progressive collapse modelling", *J. Struct. Eng.*, **137**(9), 914-924.

ASCE (2000), *Prestandard and Commentary for the Seismic Rehabilitation of Buildings - FEMA 356*, Washington D.C., USA.

Baker, J.W., Schubert, M. and Faber, M.H. (2008), "On the assessment of robustness", *Struct. Safety*, **30**(3), 253-267.

CEN (2004), EN 1998-1 - Eurocode 8 - Design of structures for earthquake resistance - Part 1: General rules, seismic actions and rules for buildings, Brussels, Belgium.

CEN (2005), EN 1993-1-1 - Eurocode 3 - Design of steel structures - Part 1-1: General rules and rules for buildings, Brussels, Belgium.

CEN (2006), EN 1991-1-7 - Eurocode 1 - Actions on structures - Part 1-7: General actions - Accidental actions, Brussels, Belgium.

Comeliau, L., Demonceau, J.F. and Jaspart, J.P. (2010), "Robustness of steel and composite buildings under impact loading", *SDSS'Rio 2010 Stability and Ductility of Steel Structures*, Rio de Janeiro, Brazil, September.

CSI (2009), CSI Analysis Reference Manual - For SAP 2000, ETABS and SAFE, CSI, Berkeley, CA, USA.

D'Aniello, M., Landolfo, R., Piluso, V. and Rizzano, G. (2012), "Ultimate behaviour of steel beams under non-uniform bending", *J. Const. Steel Res.*, **78**, 144-158.

D'Aniello, M., Güneyisi, E.M., Landolfo, R. and Mermerdaş, K. (2014), "Analytical prediction of available rotation capacity of cold-formed rectangular and square hollow section beams", *Thin-Wall. Struct.*, **77**, 141-152.

D'Aniello, M., Güneyisi, E.M., Landolfo, R. and Mermerdaş, K. (2015), "Predictive models of the flexural overstrength factor for steel thin-walled circular hollow section beams", *Thin-Wall. Struct.*, **94**, 67-78.

Dassault (2010), Abaqus 6.13 – Abaqus Analysis User's Manual.

Dassault (2013), Abaqus 6.13 – Abaqus Analysis User's Manual.

Della Corte, G., D'Aniello, M. and Landolfo, R. (2013), "Analytical and numerical study of plastic overstrength of shear links", *J. Const. Steel Res.*, **82**, 19-32.

Dinu, F., Dubina, D. and Marginean, I. (2015), "Improving the structural robustness of multi-storey steel-frame buildings", *Struct. Infrastr. Eng.*, **11**(8), 1028-1041.

El-Tawil, S., Li, H. and Kunnath, S. (2014), "Computational simulation of gravity-induced progressive collapse of steel-frame buildings: Current trends and future research needs", *J. Struct. Eng.*, **140**(8), 216-228.

Formisano, A. and Mazzolani, F.M. (2010), "On the catenary effect of steel buildings", *COST ACTION C26: Urban Habitat Constructions under Catastrophic Events - Proceedings of the Final Conference*, Naples, Italy, September, 619-624.

Formisano, A. and Mazzolani, F.M. (2012), "Progressive collapse and robustness of steel framed structures", *Proceedings of the 11th International Conference on Computational Structures Technology*, Stirlingshire, Scotland, month.

Formisano, A., Landolfo, R. and Mazzolani, F.M. (2015), "Robustness assessment approaches for steel framed structures under catastrophic events", *Comput. Struct.*, **147**, 216-228.

Fu, F. (2010), "3-D nonlinear dynamic progressive collapse analysis of multi-storey steel composite frame buildings - Parametric study", *Eng. Struct.*, **32**(12), 3974-3980.

Gerasimidis, S. (2014), "Analytical assessment of steel frames progressive collapse vulnerability to corner column loss", *J. Const. Steel Res.*, **95**, 1-9.

Gerasimidis, S. and Baniotopoulos, C. (2015), "Progressive collapse mitigation of 2D steel moment frames: assessing the effect of different strengthening schemes", *Stahlbau*, **84**(5), 324-331.

Gerasimidis, S., Deodatis, G., Kontoroupi, T. and Ettouney, M. (2014), "Loss-of-stability induced progressive collapse modes in 3D steel moment frames", *Struct. Infrastr. Eng.*, **11**(3), 334-344.

Grecea, D., Dinu, F. and Dubina, D. (2004), "Performance criteria for MR steel frames in seismic zones", *J. Const. Steel Res.*, **60**(3-5), 739-749.

GSA (2003), *Progressive Collapse Analysis and Guidelines for New Federal Office Buildings and Major Modernization Projects*.

Güneyisi, E.M., D'Aniello, M., Landolfo, R. and Mermerdaş, K. (2013), "A novel formulation of the flexural overstrength factor for steel beams", *J. Const. Steel Res.*, **90**, 60-71.

Güneyisi, E.M., D'Aniello, M., Landolfo, R. and Mermerdaş, K. (2014), "Prediction of the flexural overstrength factor for steel beams using artificial neural network", *Steel Compos. Struct., Int. J.*, **17**(3), 215-236.

Hayes, J., Woodson, S., Pekelnicky, R., Poland, C., Corley, W. and Sozen, M. (2005), "Can strengthening for earthquake improve blast and progressive collapse resistance?", *J. Struct. Eng.*, **131**(8), 1157-1177.

Izzudin, B., Vlassis, A., Elghazouli, A. and Nethercot, D. (2008), "Progressive collapse of multi-storey buildings due to sudden column loss - Part I: Simplified assessment framework", *Eng. Struct.*, **30**(5), 1308-1318.

Jahromi, H. (2009), "Progressive collapse of building structures - Influence of membrane action in floor slabs", M.Sc. Dissertation; Imperial College London, London, UK.

Khandelwal, K., El-Tawil, S., Kunnath, S. and Lew, H. (2008), "Macromodel-Based Simulation of Progressive Collapse: Steel Frame Structures", *J. Struct. Eng.*, **137**(7), 1070-1078.

Kim, T. and Kim, J. (2009), "Collapse analysis of steel moment frames with various seismic connections", *J. Const. Steel Res.*, **65**, 1316-1322.

Lalani, M. and Shuttleworth, E.P. (1990), "The ultimate state of offshore platforms using reserve and residual strength principles", *Proceedings of the 22nd Offshore Technology Conference*, Houston, TX, USA, May.

Lu, D., Cui, S., Song, P. and Chen, Z. (2012), "Robustness assessment for progressive collapse of framed structures using pushdown analysis method", *Int. J. Reliab. Saf.*, **6**(1-3), 15-37.

Ruth, P., Marchand, K. and Williamson, E. (2006), "Static equivalency in progressive collapse alternate path analysis: Reducing conservatism while retaining structural integrity", *J. Perf. Constr. Fac.*, **20**(4), 349-364.

Starossek, U. and Haberland, M. (2008), "Approaches to measures of structural robustness", *Proceedings of IABMAS'08, 4th International Conference on Bridge Maintenance, Safety and Management*, Seoul, Korea, July.

Tsai, M., and Lin, B. (2009), "Dynamic amplfication factor for progressive collapse resistance analysis of a RC building", *Struct. Des. Tall Sp. Build.*, **18**(5), 469-486.

Tartaglia, R., D'Aniello, M. and Landolfo, R. (2016), "Nonlinear performance of extended stiffened end plate bolted beam-to-column joints subjected to column removal", *Op. Civ. Eng. J.*

Tenchini, A., D'Aniello, M., Rebelo, C., Landolfo, R., da Silva, L.S. and Lima, L. (2014), "Seismic performance of dual-steel moment resisting frames", *J. Const. Steel Res.*, **101**, 437-454.

USDoD (2005), United Facilities Criteria (UFC) - Design of buildings to resist progressive collapse.

USDoD (2009), United Facilities Criteria (UFC) - Design of buildings to resist progressive collapse.

USDoD (2013), United Facilities Criteria (UFC) - Design of buildings to resist progressive collapse.

Xu, G. and Ellingwood, B. (2011), "Probabilistic assessment of pre-Northridge steel moment resisting frames", *J. Struct. Eng.*, **137**, 925-934.

CC